The Lighthouse Journal of Natural Sciences, Vol. 01, Issue 01, Summer 2022, pp. 13-20

Fabrication of Compact Films Butyl Ammonium Chloride Doping into $Cs_3Bi_2I_9$: Improved Film Morphology

Abbas Ali[1], Abdul Basit[1], Aleena Gul[1], Muhammad Junaid[2], Idrees Ahmed[2], Muhammad Usman[2], Sana Ullah[2], Nasir Ali[2], Sanam Attique[3]

ABSTRACT

Albeit the iconic lead-based perovskites solar cell has summited power conversion efficiency (PCE) of 23%. Lead toxicity remains a glitch for its commercialization. To replace the toxic lead, numerous alternatives have been introduced. Out of many, bismuth (Bi) was introduced as a stable alternative with isoelectronic properties to the conventional lead in perovskites (PVKs) framework. However, Bi-based PVKs also encountered several problems; for example, poor film morphology and crystallinity. The crystallization of Bi-based PVKs is abrupt and does not form any intermediate solvated phases, leading toward isolated crystals formation instead of uniform pinholes-free films. Hence, it is challenging to fabricate compact thin films of Bi-based PVKs. Herein, we attempted to fabricate compact and pinholes-free Bi-based PVKs film by incorporating butyl ammonium chloride (BACl) into the precursor solution of the Bi-based PVKs. Preliminary results indicate that the doping of BACl not only caused the improvement in the film morphology but also improved the crystallinity of the film. We believe that these results could be helpful in the material development of the Bi-based PVKs and their utilization in optoelectronic devices.

Keywords: *Bi-based perovskites, Butylammonium chloride, Thin film synthesis*

INTRODUCTION

Organometal halide perovskites are in demand because of their prodigious applications as ferroelectrics, piezoelectric, superconductors, photovoltaic, LED, LASER, etc. [1]. They are propitious ones for optoelectronic devices having high absorption coefficient, enhanced charged mobility, long charged diffusion length, and small exciton binding energy. In a very short period, lead-based perovskites PCE reaching 24.2% with low cost and low-temperature solution processibility made itself a strong contender against the mainstream state of art device silicon-based solar cells [2].

Besides these peculiar advantages, PVKs encountered many serious pitfalls like they are highly unstable against humidity, heat, and UV light. Owing to a long-standing impression of lead-based organometal halide perovskites' efficiency, its toxicity due to the presence of lead inhibits its commercialization. A lot of work has been done to solve the problem of moisture ingress using proper encapsulation and combining it with lower-dimensional PVK [3, 4]. The

[1] Department of Physics, Government Degree College Gul Abad, District Dir Lower, Khyber Pakhtunkhwa, Pakistan.
[2] Government Degree College Thana, District Malakand, Khyber Pakhtunkhwa, Pakistan: **Corresponding Author's Email nasirphysicist@yahoo.com**
[3] Institute for Composites Science and Innovation (InCSI), School of Material Science and Engineering, Zhejiang University, Hangzhou, PR China

Manuscript Submitted: May 10, 2022
Manuscript Accepted: June 23, 2022

Down conversion technique is used to solve the problem of UV light and thermal instability is resolved by using a 2D material at the top of the PVK layer [5, 6]. Instead of all the solutions regarding the pitfalls toxification of lead is not able to compensate as there is no safe threshold value of the damage caused by lead has been reported. High levels of health risks indulge the scientific community to dig out a possible solution to replace toxic lead with nontoxic or less toxic elements [7, 8]. In this regard, many materials have been put forward by the scientific community to find out the best replacement for lead. Mostly this replacement is from group 14 and group 15 of periodic table elements.

Prominently group 14 has mainly Sn and Ge as potential candidates for replacement of the lead. Sn is prone to self-doping [9]. Ge has its problem of smaller band gaps that are not even in the range of the Shockley-Queisser limit necessary for working of the solar cell.

Group 15 ultimate choice is Bi as it shares the same electronic configuration, comparable ionic radius, similar electronic configuration, and above all Bi is nontoxic and is used in many medicines [10, 11]. As far as toxicity and stability are concerned, Bi remained a probable choice as a lead alternative [12]. Attaining charge neutrality in typical PVKs ABX_3 structure is difficult as Bi has a different oxidation state than that of lead [13, 14]. To cope with it, mixed valency approach is used to balance the charges in the structure as the lattice of Bi-based PVKs built up of distorted octahedra due to which they have structural diversity and can be easily categorized as zero, one, two, and three-dimensional structures [15]. [16-18]. Many groups inferred that for Bi-based PVKs poor film morphology is the greatest hitch in improving the device efficiency so that it comes at par with lead-based perovskite efficiency [19, 20].

The high-quality film is a necessary aid to achieve high device performance and stability. Many approaches are being practiced to solve this glitch instantly. In this regard, films were made by using single-step and two-step spin-coating deposition techniques for compact film fabrication [16, 21]. Some groups reported solvent engineering approaches for better film morphology significant improvement in device performance has been reported by improving the film quality [19]. Though Bi-based, PVKs have superior stability factors in the open air, their poor device performance is very disheartening therefore extensive research is needed to resolve the issue of film quality by understanding what is lacking to assemble green and inexpensive solar cells.

Better PV performance needed quality thin films with full coverage, improved crystallinity, and pinhole-free films. For instance, Bi-based PVKs crystalize in a very different manner than that conventional Pb-based PVKs. It crystallizes without forming any solvated phase and grows to form an uneven isolated crystal with greater pinholes and thin films [22, 23]. Thus it's really difficult to fabricate compact pinhole-free thin films for Bi-based PVKs.

Bi has also been used as a dopant material in different materials for electrical conduction enhancement, photonic applications, etc.[24, 25]. For instance, we thought that doping may have fruitful effects on the morphology of Bi-based PVKs films. Here in this paper, we have doped $Cs_3Bi_2I_9$ with Butyl ammonium chloride followed by one-step film synthesis which gives maximum coverage on ITO substrate. Doping of Butyl ammonium chloride resulted in better compact films having excellent film morphology with improved crystallinity. These better results could be helpful in compact film fabrication and may eventually provide efficient device fabrication.

METHODOLOGY

Cesium iodide (CsI), bismuth iodide (BiI_3), butyl ammonium chloride (BACl), hydrochloric acid, dimethyl formamide (DMF), and indium tin oxide (ITO) glass substrates

were purchased from McKlin China. All of the purchased reagents were of analytical grade and used as received.

Preparation of $Cs_3Bi_2I_9$ solution: CsI and BiI_3 were dissolved completely in DMF solution with 1.5 millimolar and 1 millimolar ratio respectively under constant stirring at 70 ℃ temperature for about two hours. Filtered out the saturated solution using an organic filter after the designated time.

Preparation of doping solution: For doping CBI solution 0.1milli molar amount of butyl ammonium chloride was added to the above prepared $Cs_3Bi_2I_9$ solution to ensure that dopant dissolved and chemical reaction occurred completely doped solution kept on stirring again for about six hours. After the designated time, filter out the solution using an organic filter. Now our doped solution is ready which is further used for characterization and film fabrication.

Glass cleaning: To ensure the formation of better quality films substrate cleaning is very essential to make it free from any dust and other residues which may contaminate the film or the solution. ITO glass was sonicated (10 min) in de-ionized water, acetone and ethanol. Each time after sonication, the glass substrates were dipped in hot water (~ 90 ℃) and dried with nitrogen gas. The substrates were finally treated with UV-Ozone to remove all the organic species from the surface.

Film Fabrication: One-step spin-coated thin film fabrication is now can be done using a cleaned ITO substrate. About 70 µl of the doped solution was dropped gently at the center of the glass substrate which is already spinning at 3500rpm and after one minute of rotation substrate is now removed quickly from the spin coater and placed on a hot plate on the already spinning glass substrate (3500 rpm) and allowed to rotate for 1 minute. Afterward, the substrate was quickly transferred to the hot plate and annealed at 120 C for 5 min while covered with a glass dish.

Characterizations and techniques: Photoluminescence (PL) analysis performed using Andor SR-500i-B1 spectrograph FLS-920 and Steady/Transient fluorescence spectrometer from Edinburgh Instrument having incident radiation 535 nm. Optical absorption (OA) was done by 5000 UV–VIS-NIR spectrometer by Agilent Technologies. For film characterizations, scanning electron microscope (SEM) from Hitachi S4800 was used. X-ray diffraction (XRD) analysis was done by Empyrean Alpha-681 X-Ray Diffractometer from PANalytical. Contact angle measurement was done by CAM200 optical contact-angle meter (KSV Co.Ltd.).

DISCUSSION AND ANALYSIS

Figure 1a shows the optical absorption and PL spectra of the as-prepared pure CBI films. The characteristic absorption peak (which is associated commonly with the lower dimensional perovskites) is shown at about 650 nm. The corresponding PL spectra are also shown in the same figure. The PL peak and the absorption onset are almost at the same wavelengths, indicating a lower Stoke's shift of the material. The PL peak is broader and shows a wider full-width half maxima, indicating less coverage of the substrate as well as poor crystallinity of the pure CBI film. Similarly, Fig. 1b shows the absorption and PL characteristics of the doped CBI film. In contrast to the pure CBI, the optical absorption peak of the doped CBI is of higher intensity, showing better coverage of the film. Likewise, the PL of the doped CBI is not only sharper but more intense than the pure CBI, showing better crystallinity and fewer defects sites than the doped CBI.

The improved coverage of the substrate is also vivid from the scanning electron images of the pure and doped CBI films. Figure 1c shows the SEM image of the pure CBI thin film, exhibiting dispersed sheets (parallel to the substrate) of hexagonal shape with poor coverage of the substrate. On the other side, Fig. 1d shows SEM image of the doped CBI, which has more surface coverage than the pure CBI films. Moreover, the doped CBI crystals are oriented perpendicular to the substrate, which is favorable for better charge transport in planar-type photovoltaic devices [26]. The improved coverage of the doped CBI can be attributed to the longer chain of organic cations in the structure, which usually crystallizes slowly as compared with the inorganic Cs-based perovskites [5].

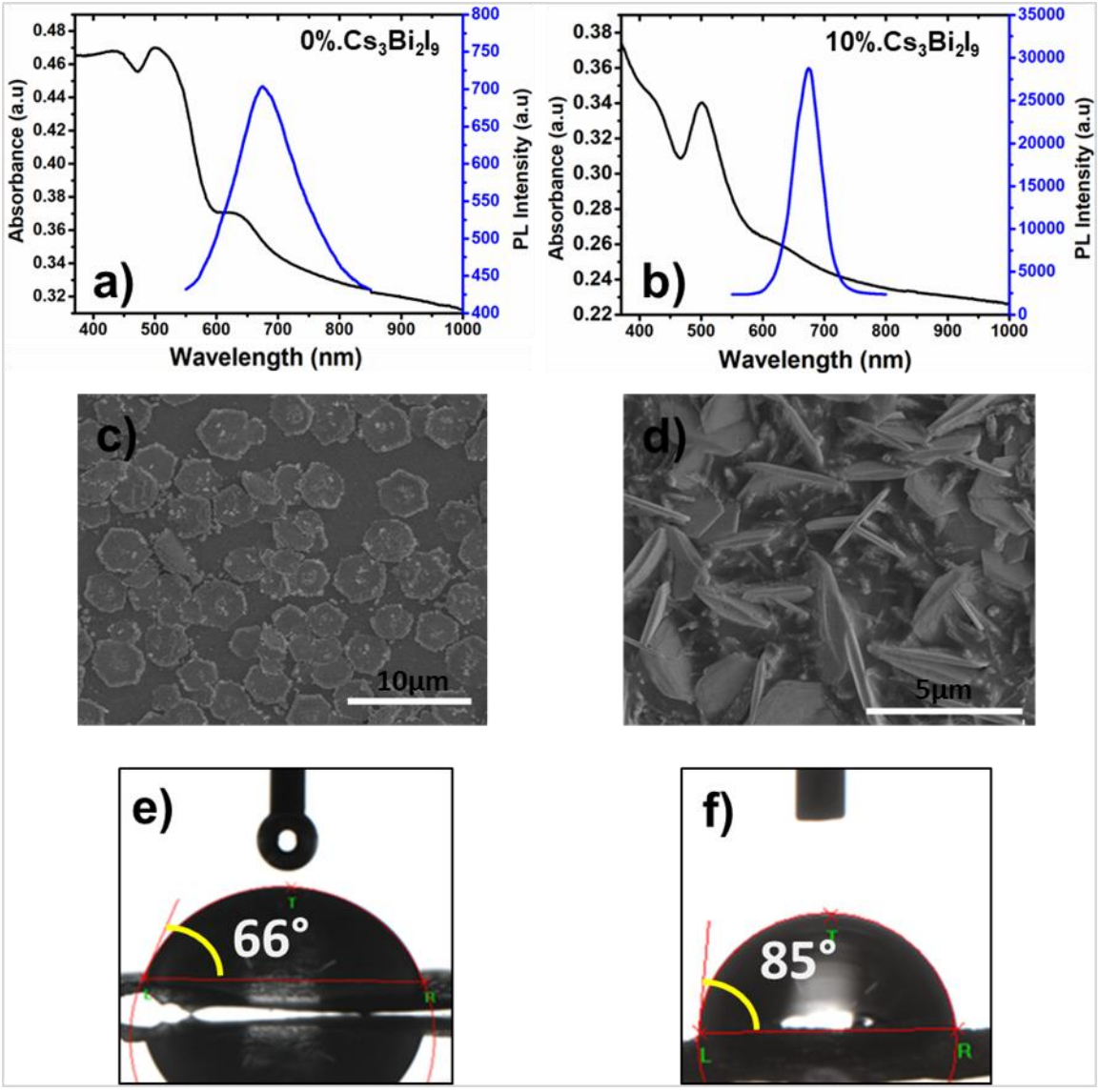

Figure 1: Optical and morphological characterization of the pure CBI and doped CBI: (**a**) absorption and PL spectra of the pure CBI. (**b**) Absorption and PL of the doped CBI. (**c**) SEM micrographs of the pure and (**d**) doped CBI thin films. (**e**) and (**f**) are the snapshots of the water contact angles respectively for the pure and doped CBI.

Additionally, to observe the surface hydrophobicity of the pure and doped CBI, water contact angle tests were performed. The water contact angle can provide information about the resistance of a material to the water ingress i.e. greater the water contact angle, the greater will

be the hydrophobicity of the material and vice versa [27]. Since doped CBI exhibited better coverage; therefore, showed a greater contact angle (85°) than the pure one (66°), as shown in Figure 1e and 1d. Better surface coverage and greater hydrophobicity could not only improve the environmental stability of the material but also for minimizing the shunt resistances of the photovoltaic device.

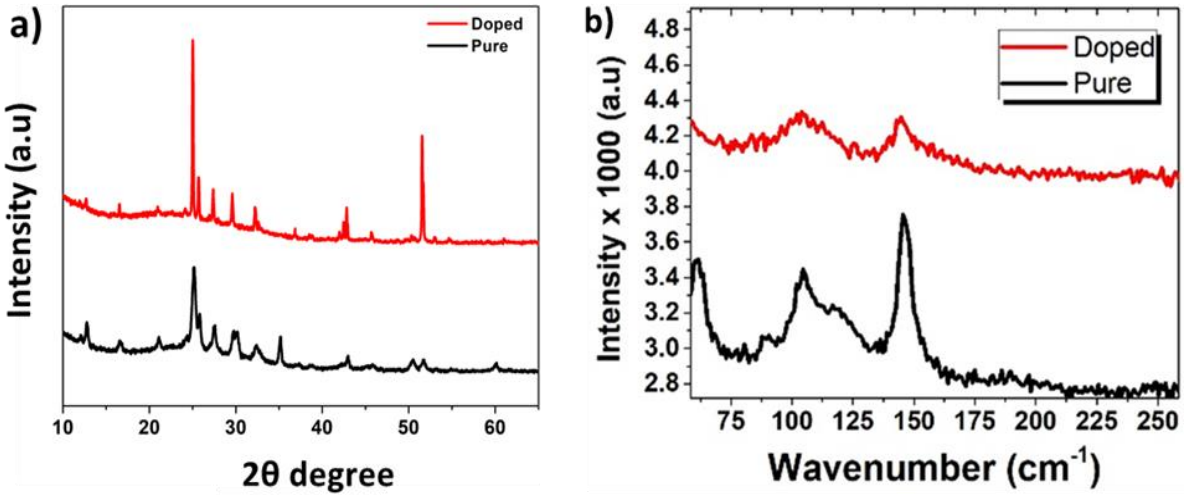

Figure 2 a) Xrd of pure and doped CBI films. **b)** Raman spectroscopy of pure and doped CBI films.

Figure 2a shows XRD spectra of pure CBI and doped CBI. Both the spectra showed a characteristic peak of hexagonal phase, i.e., Pmmc 63, which is following the previous results [28, 29]. With doping of Butyl ammonium chloride, the intensity of the XRD peaks increases. It gives more sharp peaks that are attributed to the good crystallinity of the doped CBI films. This increase in intensity is attributed to the greater film coverage, and better crystallinity as well as .pinhole-free compact films [23]. The XRD results are also in line with SEM results as well as with Raman spectra (discussed as follows).

Raman spectroscopy indicates the vibrational modes of pure CBI and doped CBI films in Figure 2b. Detailed analysis of Raman vibrational modes for CBI films has shown that $[Bi_2I_9]^{3-}$ dominates the vibrational modes in the Raman spectra. So most dominant vibrations within the structure are due to this strongly bounded anion. Major stretching in pure CBI films is shown with Bi–I mode this stretching mode is further associated with six Iodide atoms three of which are terminal iodides and the rest of the three are bridging iodides that eventually connect two Bi atoms. Peak 146 cm^{-1} for pure CBI film is the symmetric stretch whereas the two anti-symmetric stretches are shown at and two anti-symmetric stretches are shown at 127.2 cm^{-1} and 119.8 cm^{-1} [30].

Bridging iodides have a lesser force constant than that of terminal iodide atoms as they need to share their bonding with the Bi atoms to join the two Bi atoms together. The stretching peak is a high energy peak as it is related to the terminal bonds, a major peak of 146 cm^{-1} is attributed to the Bi–I terminal bonds that are associated with its anti-symmetric bonds as shown in pure CBI film [31]. Moreover, it was also attributed from Raman peaks that the presence of strong intense peaks for $[Bi_2I_9]^{3-}$ showing that still a lot of unreacted anions are still present in pure CBI film resulting in less coverage and rough film. Noticing the Raman peaks for doped CBI film showing very less intense peaks for the $[Bi_2I_9]^{3-}$ anion depicting that minute amount of anion remained unreactive and resulted in a complete chemical reaction which becomes the reason for compact and almost pin-hole free film with maximum coverage.

CONCLUSION & RECOMMENDATIONS

We have demonstrated one way to attain compact and almost pinhole-free CBI film by using the doping technique as many solvent techniques have been used to improve the quality of the film but still, poor device efficiency remained an unsolved issue because of the film quality. A comparison of pure CBI film and doped CBI film shows that organic doping has a strong impact on the quality of the film. Doping of Butyl ammonium chloride in CBI films has shown improved crystallinity, better coverage, and morphology which could be helpful in improved device efficiency. All the characterization results justify each other and are well attributed to better compact films for further utilization in optoelectronic devices.

Acknowledgment

We acknowledge funding support from the Zhejiang Provincial Natural Science Foundation of China (LR19E010001) and the National Science Foundation of China (51702283 and 51871246).

REFERENCES

1. Hirose, K., Sinmyo, R., & Hernlund, J. (2017). Perovskite in Earth's deep interior. *Science*, *358*(6364), 734-738.

2. Zhu, X., Lin, Y., San Martin, J., Sun, Y., Zhu, D., & Yan, Y. (2019). Lead halide perovskites for photocatalytic organic synthesis. *Nature communications*, *10*(1), 1-10.

3. Ali, N., Rauf, S., Kong, W., Ali, S., Wang, X., Khesro, A., ... & Wu, H. (2019). An overview of the decompositions in organo-metal halide perovskites and shielding with 2-dimensional perovskites. *Renewable and Sustainable Energy Reviews*, *109*, 160-186.

4. Attique, S., Ali, N., Khatoon, R., Ali, S., Abbas, A., Yu, Y., ... & Yang, S. (2020). Aqueous phase fabrication and conversion of Pb (OH) Br into a CH 3 NH 3 PbBr 3 perovskite and its application in resistive memory switching devices. *Green Chemistry*, *22*(11), 3608-3614.

5. Ali, N., Wang, X., Rauf, S., Attique, S., Khesro, A., Ali, S., ... & Wu, H. (2019). Enhanced stability in cesium assisted hybrid 2D/3D-perovskite thin films and solar cells prepared in ambient humidity. *Solar Energy*, *189*, 325-332.

6. Hou, J., Yu, Y., Attique, S., Cao, B., & Yang, S. (2021). Laurionite Competes with 2D Ruddlesden–Popper Perovskites During the Saturation Recrystallization Process. *ACS Applied Materials & Interfaces*, *13*(5), 6505-6514.

7. Attique, S., Ali, N., Ali, S., Khatoon, R., Li, N., Khesro, A., ... & Wu, H. (2020). A potential checkmate to lead: bismuth in organometal halide perovskites, structure, properties, and applications. *Advanced science*, *7*(13), 1903143.

8. Attique, S., Ali, N., Rauf, S., Ali, S., Khesro, A., Khatoon, R., ... & Wu, H. (2021). Nontoxic and Less Toxic Hybrid Perovskites: a Synergistic Strategy for Sustainable Photovoltaic Devices. *Solar RRL*, *5*(8), 2100212.

9. Huang, J., Gu, Z., Zhang, X., Wu, G., & Chen, H. (2018). Lead-free (CH3NH3) 3Bi2I9 perovskite `solar cells with fluorinated PDI films as organic electron transport layer. *Journal of Alloys and Compounds*, *767*, 870-876.

10. Hoye, R. L., Brandt, R. E., Osherov, A., Stevanović, V., Stranks, S. D., Wilson, M. W., ... & Buonassisi, T. (2016). Methylammonium bismuth iodide as a lead-free, stable hybrid organic–inorganic solar absorber. *Chemistry–A European Journal*, *22*(8), 2605-2610.

11.Turkevych, I., Kazaoui, S., Ito, E., Urano, T., Yamada, K., Tomiyasu, H., ... & Aramaki, S. (2017). Photovoltaic rudorffites: lead-free silver bismuth halides alternative to hybrid lead halide perovskites. *ChemSusChem*, *10*(19), 3754-3759.

12. Brandt, R. E., Stevanović, V., Ginley, D. S., & Buonassisi, T. (2015). Identifying defect-tolerant semiconductors with high minority-carrier lifetimes: beyond hybrid lead halide perovskites. *Mrs Communications*, *5*(2), 265-275.

13. Wang, Z., Shi, Z., Li, T., Chen, Y., & Huang, W. (2017). Stability of perovskite solar cells: a prospective on the substitution of the A cation and X anion. *Angewandte Chemie International Edition*, *56*(5), 1190-1212.

14. Yang, B., Chen, J., Hong, F., Mao, X., Zheng, K., Yang, S., ... & Han, K. (2017). Lead-free, air-stable all-inorganic cesium bismuth halide perovskite nanocrystals. *Angewandte Chemie International Edition*, *56*(41), 12471-12475.

15. Creutz, S. E., Liu, H., Kaiser, M. E., Li, X., & Gamelin, D. R. (2019). Structural diversity in cesium bismuth halide nanocrystals. *Chemistry of Materials*, *31*(13), 4685-4697.

16. Park, B. W., Philippe, B., Zhang, X., Rensmo, H., Boschloo, G., & Johansson, E. M. (2015). Bismuth based hybrid perovskites A3Bi2I9 (A: methylammonium or cesium) for solar cell application. *Advanced materials*, *27*(43), 6806-6813.

17. Johansson, M. B., Zhu, H., & Johansson, E. M. (2016). Extended photo-conversion spectrum in low-toxic bismuth halide perovskite solar cells. *The journal of physical chemistry letters*, *7*(17), 3467-3471.

18. Singh, T., Kulkarni, A., Ikegami, M., & Miyasaka, T. (2016). Effect of electron transporting layer on bismuth-based lead-free perovskite (CH3NH3) 3 Bi2I9 for photovoltaic applications. *ACS applied materials & interfaces*, *8*(23), 14542-14547.

19. Shin, S. S., Correa Baena, J. P., Kurchin, R. C., Polizzotti, A., Yoo, J. J., Wieghold, S., ... & Buonassisi, T. (2018). Solvent-engineering method to deposit compact bismuth-based thin films: mechanism and application to photovoltaics. *Chemistry of Materials*, *30*(2), 336-343.

20. Mali, S. S., Kim, H., Kim, D. H., & Kook Hong, C. (2017). Anti-Solvent Assisted Crystallization Processed Methylammonium Bismuth Iodide Cuboids towards Highly Stable Lead-Free Perovskite Solar Cells. *ChemistrySelect*, *2*(4), 1578-1585.

21.Ran, C., Wu, Z., Xi, J., Yuan, F., Dong, H., Lei, T., ... & Hou, X. (2017). Construction of compact methylammonium bismuth iodide film promoting lead-free inverted planar heterojunction organohalide solar cells with open-circuit voltage over 0.8 V. *The journal of physical chemistry letters*, *8*(2), 394-400.

22 Tang, M. C., Barrit, D., Munir, R., Li, R., Barbé, J. M., Smilgies, D. M., ... & Amassian, A. (2019). Bismuth-Based Perovskite-Inspired Solar Cells: In Situ Diagnostics Reveal Similarities and Differences in the Film Formation of Bismuth-and Lead-Based Films. *Solar RRL*, *3*(7), 1800305..

23. Ali, N., Attique, S., Rauf, S., Wang, X., Khesro, A., Ali, S., ... & Wu, H. (2020). The effect of dodecylammonium chloride on the film morphology, crystallinity, and performance of lead-free Bi-based solution-processed photovoltaics devices. *Solar Energy*, *207*, 1356-1363.

24. Acharya, M., & Maiti, T. (2018). Effect of bismuth doping on thermoelectric properties of Sr2 TiCoO6. *Ferroelectrics*, *532*(1), 28-37.

25. Wei, S., Ding, M., Fan, D., Luo, Y., Wen, J., & Peng, G. D. (2018). Effects of post treatments on bismuth-doped and bismuth/erbium co-doped optical fibres. *Bismuth: Advanced Applications and Defects Characterization*, *155*.

26. Bi, C., Shao, Y., Yuan, Y., Xiao, Z., Wang, C., Gao, Y., & Huang, J. (2014). Understanding the formation and evolution of interdiffusion grown organolead halide perovskite thin films by thermal annealing. *Journal of Materials Chemistry A*, *2*(43), 18508-18514.

27. Ma, Y., Cao, X., Feng, X., Ma, Y., & Zou, H. (2007). Fabrication of super-hydrophobic film from PMMA with intrinsic water contact angle below 90. *Polymer*, *48*(26), 7455-7460.

28. Park, B. W., Philippe, B., Zhang, X., Rensmo, H., Boschloo, G., & Johansson, E. M. (2015). Bismuth based hybrid perovskites A3Bi2I9 (A: methylammonium or cesium) for solar cell application. *Advanced materials*, *27*(43), 6806-6813.

29. Zhang, H., Xu, Y., Sun, Q., Dong, J., Lu, Y., Zhang, B., & Jie, W. (2018). Lead free halide perovskite Cs 3 Bi 2 I 9 bulk crystals grown by a low temperature solution method. *CrystEngComm*, *20*(34), 4935-4941.

30. McCall, K. M., Stoumpos, C. C., Kostina, S. S., Kanatzidis, M. G., & Wessels, B. W. (2017). Strong electron–phonon coupling and self-trapped excitons in the defect halide perovskites A3M2I9 (A= Cs, Rb; M= Bi, Sb). *Chemistry of Materials*, *29*(9), 4129-4145.

31. Laane, J., & Jagodzinski, P. W. (1980). Low-frequency vibrational spectra of bromo-and iodobismuthates and the observation of a trans effect. *Inorganic Chemistry*, *19*(1), 44-49.